Supporting Information

Small Molecule Acceptor with Heptacyclic Benzodi(thienocyclopentafuran) Central Unit Achieving a 13.4% Efficiency in Polymer Solar Cells with Low Energy Loss

Kun Wang,[ab] Juan Chen,[a] Jun Hu,[a] Xia Guo,[a] Maojie Zhang,[a]* Yongfang Li[ac]*

[a] Laboratory of Advanced Optoelectronic Materials, College of Chemistry, Chemical Engineering and Materials Science, Soochow University, Suzhou 215123, China

E-mail: mjzhang@suda.edu.cn; guoxia@suda.edu.cn

[b] K. Wang

School of Materials and Chemical Engineering, Zhongyuan University of Technology, Zhengzhou 451191, China.

[c] Prof. Y. F. Li

Beijing National Laboratory for Molecular Sciences, CAS Key Laboratory of Organic Solids, Institute of Chemistry, Chinese Academy of Sciences, Beijing 100190, China

K. Wang and J. Chen contributed equally to this work

Experimental section

Materials.

All chemicals and solvents were reagent grades and purchased from Alfa Aesar, J&K, Aldrich and TCI Chemical et al. BDF was synthesized according to previously reported literature. [1,2] PM6 was synthesized according to the procedure we reported before, the number-average molecular weight (M_n), weight-average molecular weight (M_w) and the polydispersity index (PDI) are 21.4 kDa, 64.66 kDa and 3.02, respectively. [3] The synthetic route of small molecule acceptor BFHIC and BFHIC-4F are shown in **Scheme** S**1**, the detailed synthetic processe as follows:

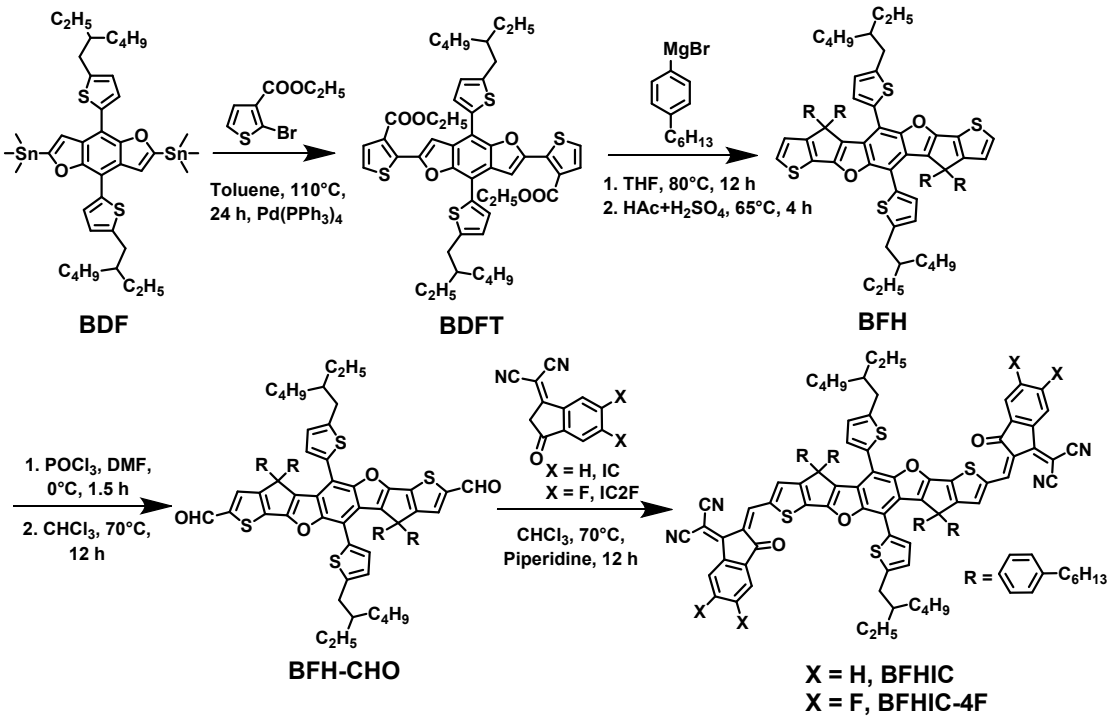

Scheme S1 The synthetic route and molecular structure of BFHIC and BFHIC-4F.

Synthesis of compound **BDFT**: Compound BDF (2.93 g, 3.36 mmol), ethyl 2-bromothiophene-3-carboxylate (2.37 g, 10.08 mmol), and 130 mL toluene were added into a 250 mL two-necked round-bottom flask. The mixture was deoxygenated with argon for 20 min, then $Pd(PPh_3)_4$ (0.31 g, 0.369 mmol) was added under argon. The mixture was refluxed at 110 °C for 24 h and then cooled down to room temperature. Water (100 mL) was added and the mixture was extracted with dichloromethane (CH_2Cl_2) (120 mL). The organic phase was dried over anhydrous $MgSO_4$ and filtered. After the removal of solvent, purification was carried out by silica gel column chromatography using petroleum ether/CH_2Cl_2 (v/v = 3:1) as the eluent yielding a yellow solid BDFT (2.5 g, 73%). ^{1}H NMR (400 MHz, $CDCl_3$), δ (ppm): 8.43 (s, 2H), 7.81-7.80 (d, 2H), 7.59-7.58 (d, 2H), 7.34-7.32 (d, 2H), 6.95-6.94 (d, 2H), 4.44-4.39 (m, 4H), 2.91-2.89 (d, 4H), 1.73-1.70 (t, 2H), 1.51-1.26 (m, 16H), 0.98-0.92 (m, 18H). ^{13}C NMR (400 MHz, $CDCl_3$), δ (ppm): 163.00, 149.63, 148.76, 147.87, 145.42, 144.99, 138.91, 134.10, 133.82, 131.00, 128.05, 127.72, 127.47, 125.77, 125.74, 124.91, 124.61, 123.77, 110.57, 109.54, 108.44, 107.36, 60.92, 41.46, 34.16, 34.09,

32.45, 31.59, 29.70, 28.93, 25.57, 25.55, 23.06, 22.66, 14.36, 14.20, 14.18, 14.03, 10.92, 10.87. MALDI-TOF MS: calcd. For $C_{48}H_{54}O_6S_4$ m/z=854.28; found 854.38.

Synthesis of compound **BFH**: To a three-necked round bottom flask were added compound BDFT (1 g, 1.17 mmol) and dry THF (20 mL). Then the THF solution (20 mL) of fresh 4-hexylphenyl-1-magnesium bromide which prepared from magnesium turnings (0.281 g, 11.7 mmol) and 1-bromo-4-hexylbenzene (2.82 g, 11.7 mmol) (Iodine as an initiator) was added dropwise to the mixture. The mixture was refluxed for 12 h, and then cooled down to room temperature. A saturated NH_4Cl aqueous solution was added and the mixture was extracted with CH_2Cl_2 (3 ×50 mL). The organic phase was dried over anhydrous $MgSO_4$ and filtered. After removing the solvent, the residue was dissolved in 300 mL n-octane, then the mixture of acetic acid (29 mL) and sulfuric acid (0.6 mL) was added drop by drop under the protection of argon. The mixture was refluxed at 65 °C for 4 h, then cooled down to room temperature and extracted with trichloromethane ($CHCl_3$) (120 mL). The organic phase was dried over anhydrous $MgSO_4$. After the removal of solvent, purification was carried out by silica gel column chromatography using petroleum ether as the eluent yielding a yellow viscous compound BFH (0.75 g, 60%). ^{1}H NMR (400 MHz, $CDCl_3$), δ (ppm): 7.56-7.54 (d, 2H), 7.17 (d, 2H), 7.11-7.09 (d, 4H), 6.91-6.89 (d, 4H), 6.73-6.69 (m, 4H), 5.94-5.93 (d, 4H), 5.36-5.28 (m, 4H), 2.90-2.85 (m, 4H), 2.59-2.53 (m, 22H), 1.43-1.27 (m, 36H), 0.96-0.86 (m, 24H). MALDI-TOF MS: calcd. For $C_{92}H_{110}O_2S_4$ m/z=1375.74; found 1375.96.

Synthesis of compound **BFH-CHO**: Compound $POCl_3$ (1.32 mL, 14.16 mmol), were added into a 100 mL two-necked round-bottom flask under argon protection. The solution was cooled to 0 ^{o}C and stirred when 1.36 ml DMF was added by syringe. The mixture was stirred for 1.5 h, and then compound BFH (1.08 g, 1.77 mmol) in $CHCl_3$ (30 ml) was added. Then, the mixture solution was allowed to reflux 12 h. After cooling to room temperature, the mixture was extracted with CH_2Cl_2, and the organic layer was collected, dried with anhydrous $MgSO_4$. After removal of the solvent under reduced pressure, the residue was purified by column chromatography on silica gel using petroleum ether/CH_2Cl_2 (v/v=1/1) as eluent to give an orange solid

(0.99 mg, 88%). ^{1}H NMR (400 MHz, $CDCl_3$), δ (ppm): 9.72 (s, 2H), 7.47 (s, 2H), 6.97-6.95 (d, 8H), 6.88-6.86 (d, 8H), 6.38 (s, 2H), 6.01 (s, 2H), 2.76-2.75 (d, 4H), 2.57-2.53 (t, 8H), 1.32-1.30 (m, 50H), 0.94-0.87 (m, 24H). ^{13}C NMR (400 MHz, $CDCl_3$), δ (ppm): 182.65, 163.75, 146.29, 145.34, 141.90, 139.03, 138.30, 136.02, 130.72, 129.82, 128.26, 128.15, 125.02, 122.95, 109.99, 41.20, 35.49, 33.94, 32.28, 31.72, 31.43, 29.31, 29.00, 28.79, 27.19, 25.39, 23.12, 22.62, 14.25, 14.11, 10.79. MALDI-TOF MS: calcd. For $C_{94}H_{110}O_4S_4$ m/z=1430.73; found 1431.64.

Synthesis of compound **BFHIC**: Compound BFH-CHO (0.18 g, 0.126 mmol), IC (0.23 g, 1.06 mmol), and 30 mL $CHCl_3$ were added into a 50 mL two-necked round-bottom flask. Then, 1 mL pyridine was added under the protection of argon. The mixture was stirred at 65 ^{o}C for 12 h. After cooling down to room temperature, the mixture was poured into methanol (100 mL) and filtered. The residue was purified by column chromatography on silica gel using petroleum ether/CH_2Cl_2 (1:1) as eluent yield a dark green solid (0.12 mg, 80%). ^{1}H NMR (400 MHz, $CDCl_3$), δ (ppm): 8.78 (s, 2H), 8.66-8.64 (d, 2H), 7.88-7.87 (d, 2H), 7.71 (s, 4H), 7.48 (s, 2H), 7.00-6.98 (d, 8H), 6.91-6.89 (d, 8H), 6.39 (s, 2H), 5.99 (s, 2H), 2.80-2.79 (d, 4H), 2.58-2.55 (t, 8H), 1.59-1.55 (d, 16H), 1.36-1.30 (d, 32H), 0.98-0.88 (m, 24H). ^{13}C NMR (400 MHz, $CDCl_3$), δ (ppm): 188.38, 164.59, 160.15, 157.65, 157.01, 146.64, 142.41, 142.15, 140.92, 139.90, 136.78, 135.61, 134.27, 130.13, 130.10, 128.39, 128.20, 125.12, 123.54, 121.66, 114.72, 112.86, 68.45, 60.54, 41.13, 35.51, 33.87, 32.37, 31.73, 31.43, 29.31, 29.02, 28.85, 25.42, 23.19, 22.62, 14.29, 14.12, 10.78. MALDI-TOF MS: calcd. For $NC_{118}H_{118}N_4O_4S_4$ m/z=1783.81; found 1784.62.

Synthesis of compound **BFHIC-4F**: The method of synthesis and purification of BFHIC-4F was consistent with that of BFHIC, and 0.15 g dark green solid was obtained (yield 89%). ^{1}H NMR (400 MHz, $CDCl_3$), δ (ppm): 8.76 (s, 2H), 8.52-8.48 (m, 2H), 7.65-7.62 (t, 2H), 7.49 (s, 4H), 7.00-6.98 (d, 8H), 6.89-6.88 (d, 8H), 6.40-6.39 (d, 4H), 6.00-5.99 (d, 4H), 2.80-2.78 (d, 4H), 2.58-2.54 (t, 8H), 1.58-1.55 (m, 28H), 1.35-1.30 (m, 36H), 0.98-0.86 (m, 24H). ^{13}C NMR (400 MHz, $CDCl_3$), δ (ppm): 185.98, 164.87, 158.00, 157.61, 147.14, 146.78, 143.10, 142.26, 140.83, 138.14, 135.42, 130.16, 129.94, 128.42, 128.18, 125.13, 123.70, 114.32, 114.24,

113.07, 68.97, 60.59, 41.16, 35.49, 32.37, 31.71, 31.40, 29.00, 28.85, 25.45, 23.17, 22.60, 14.20, 14.09, 10.78. MALDI-TOF MS: calcd. For $NC_{118}H_{118}F_4N_4O_4S_4$ m/z=1855.77; found 1856.36.

Instruments and measurements.

UV-Vis absorption spectra were measured by an Agilent Carry-5000 UV-Vis spectrophotometer. Electrochemical cyclic voltammetry (CV) was performed on a Zahner Zennium IM6 electrochemical workstation with a three-electrode system in 0.1 mol L^{-1} Bu_4NPF_6 acetonitrile solutions at a scan rate of 50 mV s^{-1}. Thermogravimetric analysis (TGA) was measured on Discovery TGA from TA Instruments Inc. at a heating rate of 10 ^oC min^{-1} under a nitrogen atmosphere. Differential scanning calorimetry (DSC) was performed on a TA DSC Q-200 at a scan rate of 10 ^oC min^{-1} under nitrogen atmosphere, and the DSC curves are from the second run data. Photoluminescence (PL) spectra were performed on an Edinburgh Instrument FLS 980. The atomic force microscopy (AFM) measurement was carried out on a Dimension 3100 (Veeco) Atomic Force Microscope in the tapping mode. Transmission electron microscopy (TEM) was performed on a Tecnai G2 F20 S-TWIN instrument at 200 kV accelerating voltage. The current-voltage (*J-V*) characteristics of the devices were measured on a Keithley 2450 Source Measure Unit. The power conversion efficiency of the PSCs was measured under an illumination of AM 1.5G (100 mW cm^{-2}) using a SS-F5-3A (Enli Technology Co. Ltd.) solar simulator (AAA grade, 50 mm x 50 mm photobeam size). The EQE was measured by Solar Cell Spectral Response Measurement System QE-R3011 (Enli Technololy Co. Ltd.). The light intensity at each wavelength was calibrated with a standard single-crystal Si photovoltaic cell.

Photovoltaic devices fabrication

The PSCs devices were fabricated with the structure of ITO/ZnO-NPs/PFN-Br/PM6:Acceptors/MoO_3 (10 nm)/Al (100 nm). The ITO-coated glass substrate was cleaned with deionized water, acetone, and isopropanol, respectively. Subsequently,

the pre-cleaned ITO-coated glass substrate was treated by UV-ozone for 20 min. Then, the ZnO nanoparticles (ZnO-NPs) were spin-coated onto the ITO-coated glass surface at a spinning rate of 3000 *rpm* for 30 s. The ZnO-NPs was prepared according to the previous literature. [4] Then the solution of PFN-Br which was dissolved in methanol with concentration of 0.5 mg mL^{-1} was spin-coated on the surface of ZnO-coated ITO with 3000 *rpm* for 30 s. The active layer was deposited onto the ZnO layer by spin-coating a CB solution of PM6:Acceptors with PM6 concentration of 10 mg mL^{-1} inside a nitrogen box containing less than 5 ppm oxygen and moisture. Finally, 10 nm MoO_3 and 100 nm Al were sequentially evaporated on the active layer in the vacuum chamber under a pressure of ca. 4×10^{-4} Pa.

Mobility measurement

The mobility was measured by the space charge limited current (SCLC) method by a hole-only device with a structure of ITO/PEDOT:PSS/PM6:Acceptors/MnO_3(10 nm)/Al(100 nm) or an electron-only device with a structure of ITO/ZnO-NP/PM6:Acceptors or pure acceptor/PFN-Br/Al(100 nm) and estimated through the Mott-Gurney equation. For the hole-only devices, SCLC is described by $J \cong (9/8)\varepsilon\varepsilon_0\mu_0 V^2 \exp(0.89\sqrt{V/E_0 L})/L^3$, Where ε is the dielectric constant of PM6:Acceptors, ε_0 is the permittivity of the vacuum, μ_0 is the zero-field mobility, E_0 is the characteristic field, J is the current density, L is the thickness of the films, $V = V_{appl} - V_{bi}$, V_{appl} is the applied potential, and V_{bi} is the built-in potential which results from the difference in the work function of the anode and the cathode (in this device structure, V_{bi} = 0.2 V).

For the electron-only devices, SCLC is described by $J = \frac{8}{9}\varepsilon_r\varepsilon_0\mu_e\frac{V^2}{L^3}$, where J is the current density, ε_r is the dielectric constant of BFHIC-4F or BFHIC, ε_0 is the permittivity of the vacuum, L is the thickness of the blend film, $V = V_{appl} - V_{bi}$, V_{appl} is the applied potential, and V_{bi} is the built-in potential which results from the difference in the work function of the anode and the cathode (in this device structure, V_{bi} = 0 V).

TEM characterization.

TEM was measured by Tecnai G2 F20 STWIN instrument (accelerating voltage, 200 kV), where the PM6:acceptor films were prepared as follow: the PM6:acceptor films were spin coated on the PEDOT:PSS-based substrates and then were immersed in

deionized water to obtain floated BHJ films, and finally unsupported 200 mesh copper grids was used to pick films up.

Characterization of material properties

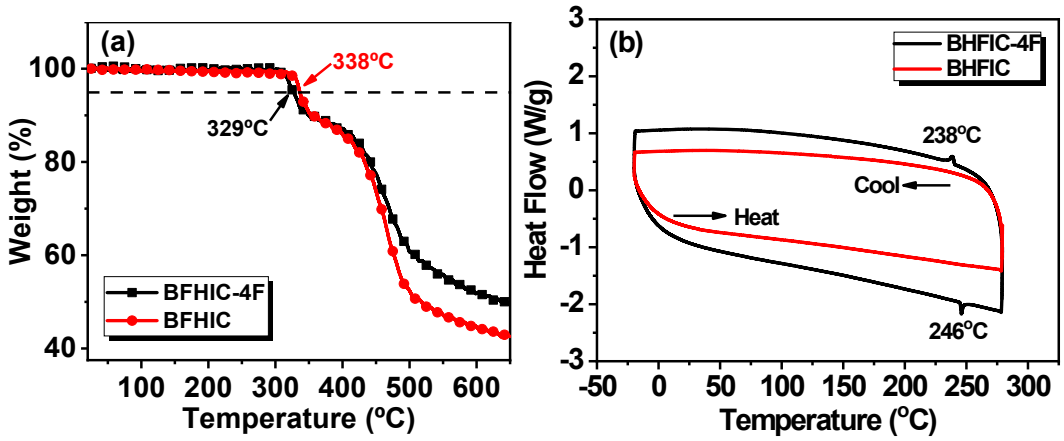

Fig. S1 TGA (a) and DSC (b) curves of BFHIC-4F and BFHIC under nitrogen atmosphere.

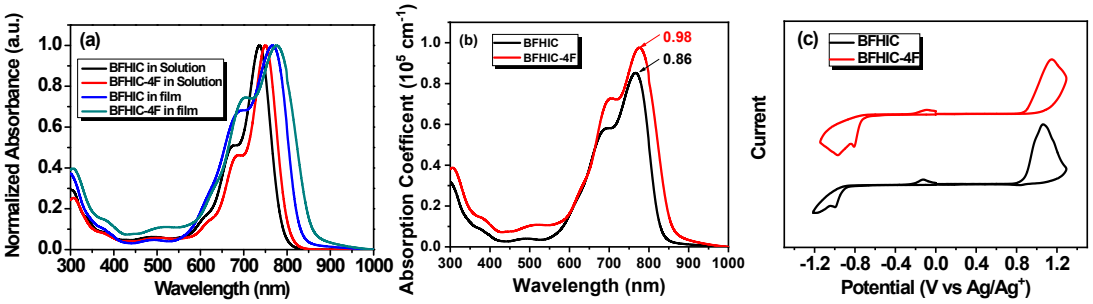

Fig. S2 (a) UV-vis absorption spectra of BFHIC-4F and BFHIC in toluene solution, and in thin film; (b) Absorption coefficent of BFHIC-4F and BFHIC in solid film; (c) Cyclic voltammogram of BFHIC-4F and BFHIC films.

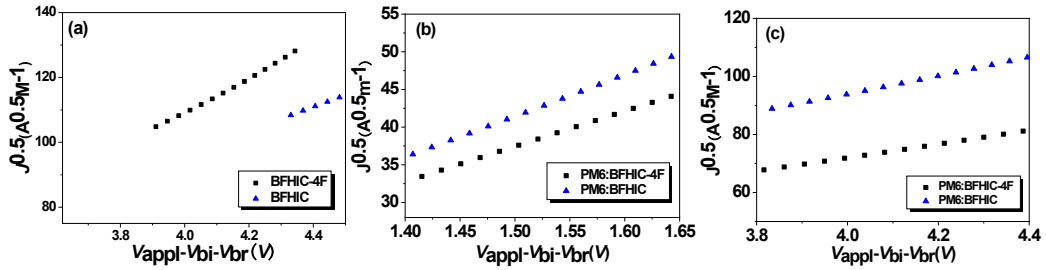

Fig. S3 $J^{0.5}$ *vs* V plots of (a) the electron-only devices with the structure of ITO/ZnO/small molecule acceptors/PFN/Al, (b) the hole-only devices with the

structure of ITO/PEDOT:PSS/active layer/MoO_3/Al, and (c) the electron-only devices with the structure of ITO/ZnO/active layer/PFN/Al according to the SCLC model.

Table S1 Charge mobilities measured by SCLC method.

Materials	Hole-mobility (μ_h) ($cm^2\ V^{-1}\ s^{-1}$)	Electron-mobility (μ_e) ($cm^2\ V^{-1}\ s^{-1}$)	μ_h/μ_e
BFHIC-4F		6.20×10^{-4}	
BFHIC		2.72×10^{-4}	
PM6:BFHIC-4F	1.85×10^{-3}	5.89×10^{-4}	3.1
PM6:BFHIC	1.64×10^{-3}	3.06×10^{-4}	5.4

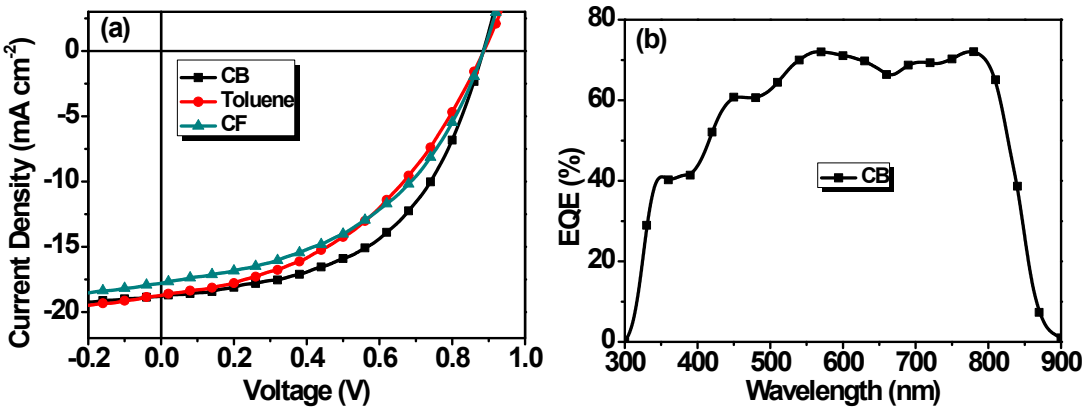

Fig. S4 (a) *J-V* curves of the PSCs based on PM6:BFHIC-4F with different solvent at D/A weight ratios of 1:1 under the illumination of AM 1.5G, 100 mW cm^{-2}. (b) The EQE curves of the device processing with CB.

Table S2 Photovoltaic parameters of the PSCs based on PM6:BFHIC-4F with different solvent at D/A weight ratio of 1:1 under the illumination of AM1.5G (100 mW cm^{-2}).

Solvent	V_{oc} (V)	J_{sc} (mA cm^{-2})	FF (%)	PCE (%)

CB	0.88	18.8	51.9	8.6
Toulene	0.89	18.7	43.9	7.3
CF	0.89	17.8	46.3	7.3

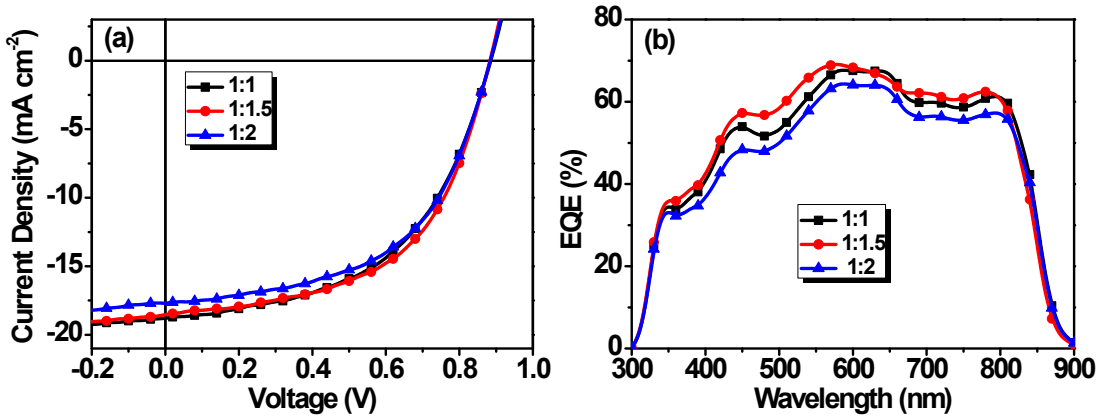

Fig. S5 (a) *J-V* curves of the PSCs based on PM6:BFHIC-4F with different D/A weight ratios at pre-optimization conditions under the illumination of AM 1.5G, 100 mW cm^{-2}. (b) The corresponding EQE curves of the devices.

Table S3 Photovoltaic parameters of the PSCs based on PM6:BFHIC-4F with different D/A weight ratios at pre-optimization conditions under the illumination of AM1.5G (100 mW cm^{-2}).

D/A (w/w)	V_{oc} (V)	J_{sc} (mA cm^{-2})	FF (%)	PCE (%)
1:1	0.88	18.8	51.9	8.6
1:1.5	0.88	18.5	55.0	9.0
1:2	0.88	17.7	53.9	8.5

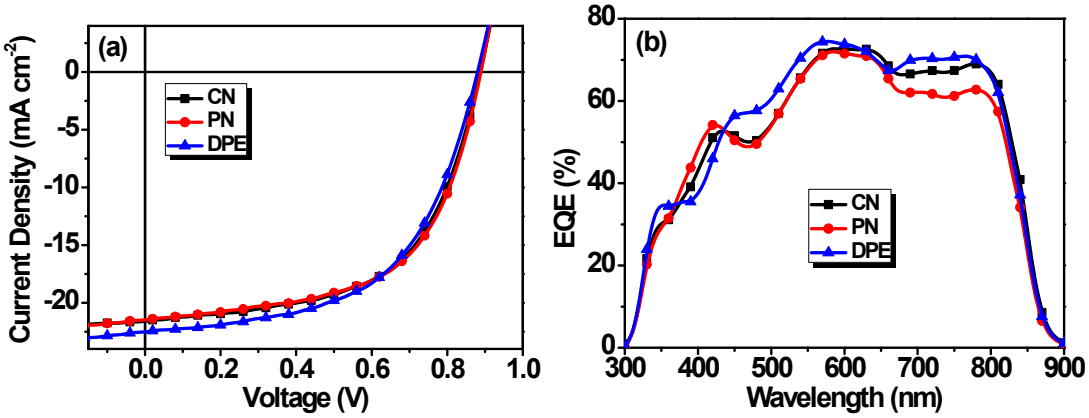

Fig. S6 (a) *J-V* curves of the PSCs based on PM6:BFHIC-4F with different additive (v/v, 0.5%) at pre-optimization conditions under the illumination of AM 1.5G, 100 mW cm^{-2}. (b) The corresponding EQE curves of the devices.

Table S4 Photovoltaic parameters of the PSCs based on PM6:BFHIC-4F with different additive at pre-optimization conditions under the illumination of AM1.5G (100 mW cm^{-2}).

Additive	V_{oc} (V)	J_{sc} (mA cm^{-2})	FF (%)	PCE (%)
0.5% CN	0.89	21.6	58.0	11.1
0.5% PN	0.89	21.5	58.7	11.2
0.5% DPE	0.88	22.5	55.7	11.1

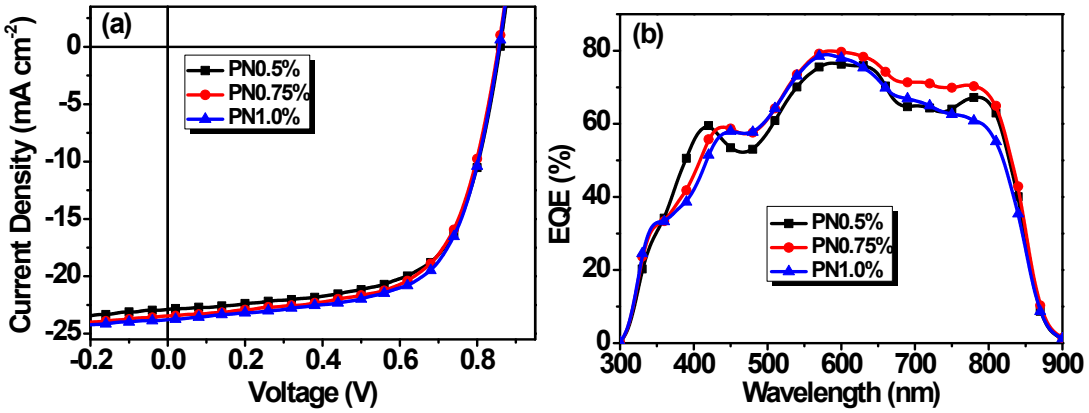

Fig. S7 (a) *J-V* curves of the PSCs based on PM6:BFHIC-4F with different additive ratios at pre-optimization conditions under the illumination of AM 1.5G, 100 mW cm^{-2}. (b) The corresponding EQE curves of the devices.

Table S5 *J-V* curves of the PSCs based on PM6:BFHIC-4F with different additive ratios at pre-optimization conditions under the illumination of AM 1.5G, 100 mW cm^{-2}.

Additive (PN)	V_{oc} (V)	J_{sc} (mA cm^{-2})	FF (%)	PCE (%)
0.5%	0.86	22.9	65.0	12.8
0.75%	0.86	23.3	64.9	13.0
1.0%	0.85	23.9	64.4	13.0

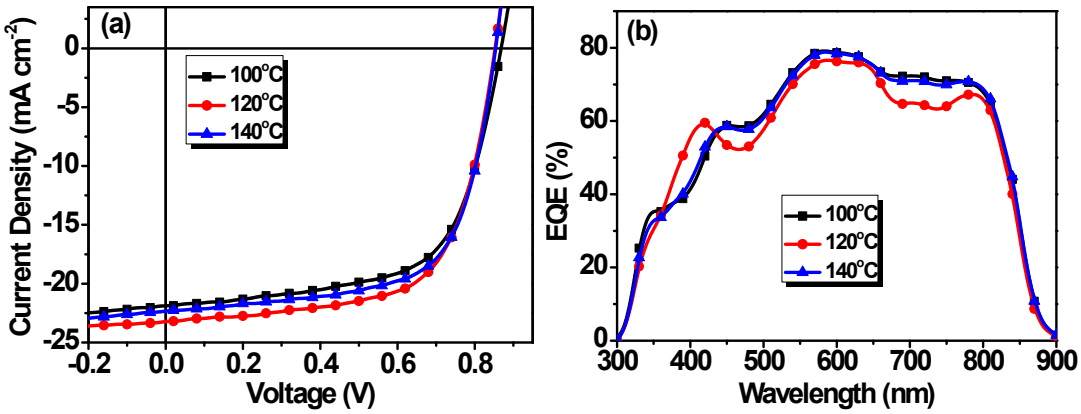

Fig. S8 (a) *J-V* curves of the PSCs based on PM6:BFHIC-4F with different TA temperature at pre-optimization conditions under the illumination of AM 1.5G, 100 mW cm^{-2}. (b) The corresponding EQE curves of the devices.

Table S6 Photovoltaic parameters of the PSCs based on PBSF-A12:IT-4F with different TA temperature at pre-optimization conditions under the illumination of AM1.5G (100 mW cm^{-2}).

TA temperature	V_{oc} (V)	J_{sc} (mA cm^{-2})	FF (%)	PCE (%)
100ºC	0.87	21.9	63.6	12.1
120ºC	0.86	23.3	64.9	13.0
140ºC	0.85	22.3	66.0	12.6

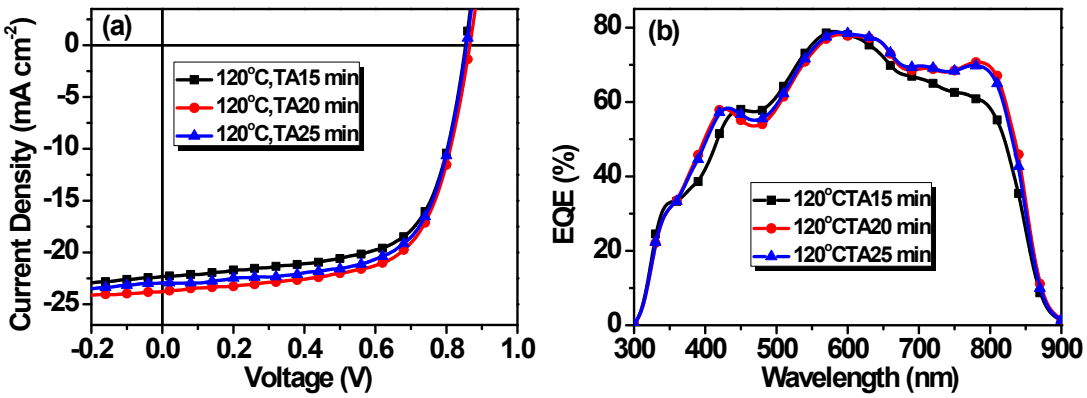

Fig. S9 (a) *J-V* curves of the PSCs based on PM6:BFHIC-4F with different TA time at pre-optimization conditions under the illumination of AM 1.5G, 100 mW cm^{-2}. (b) The corresponding EQE curves of the devices.

Table S7 Photovoltaic parameters of the PSCs based on PM6:BFHIC-4F with different TA time at pre-optimization conditions under the illumination of AM1.5G (100 mW cm^{-2}).

TA Time (min)	V_{oc} (V)	J_{sc} (mA cm^{-2})	FF (%)	PCE (%)
15	0.85	22.5	66.5	12.8
20	0.87	22.8	67.7	13.4
25	0.85	23.0	65.0	12.8

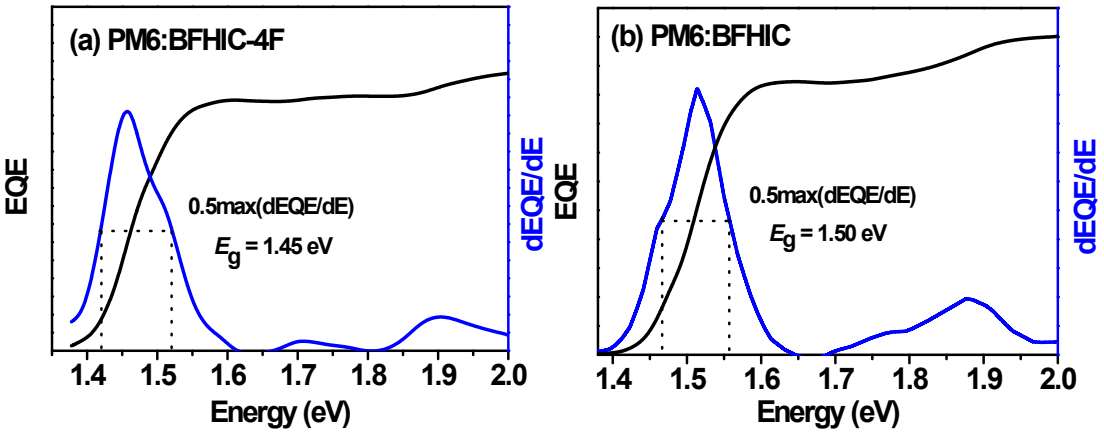

Fig. S10 Deduction of photovoltaic bandgap from the definition of E_g (a) PM6:BFHIC-4F, (b) PM6:BFHIC.

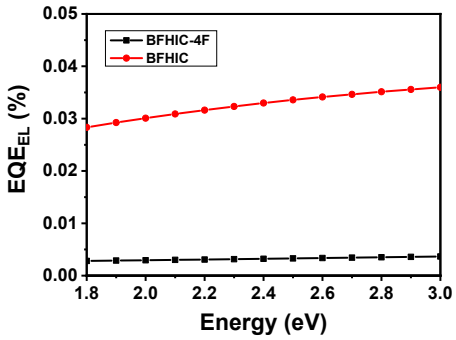

Fig. S11 Electroluminescence external quantum efficiency of the devices.

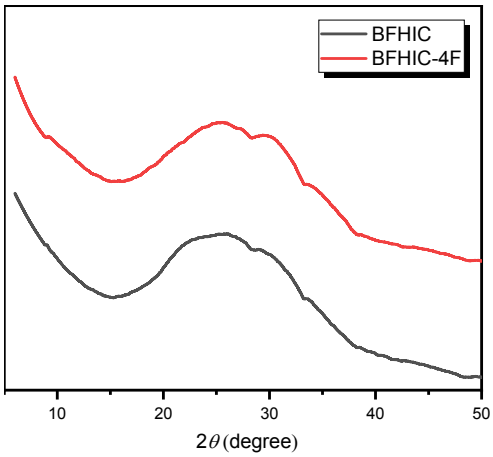

Fig. S12. X-ray diffraction patterns of BFHIC-4F and BFHIC film casted from $CHCl_3$ onto Si substrates.

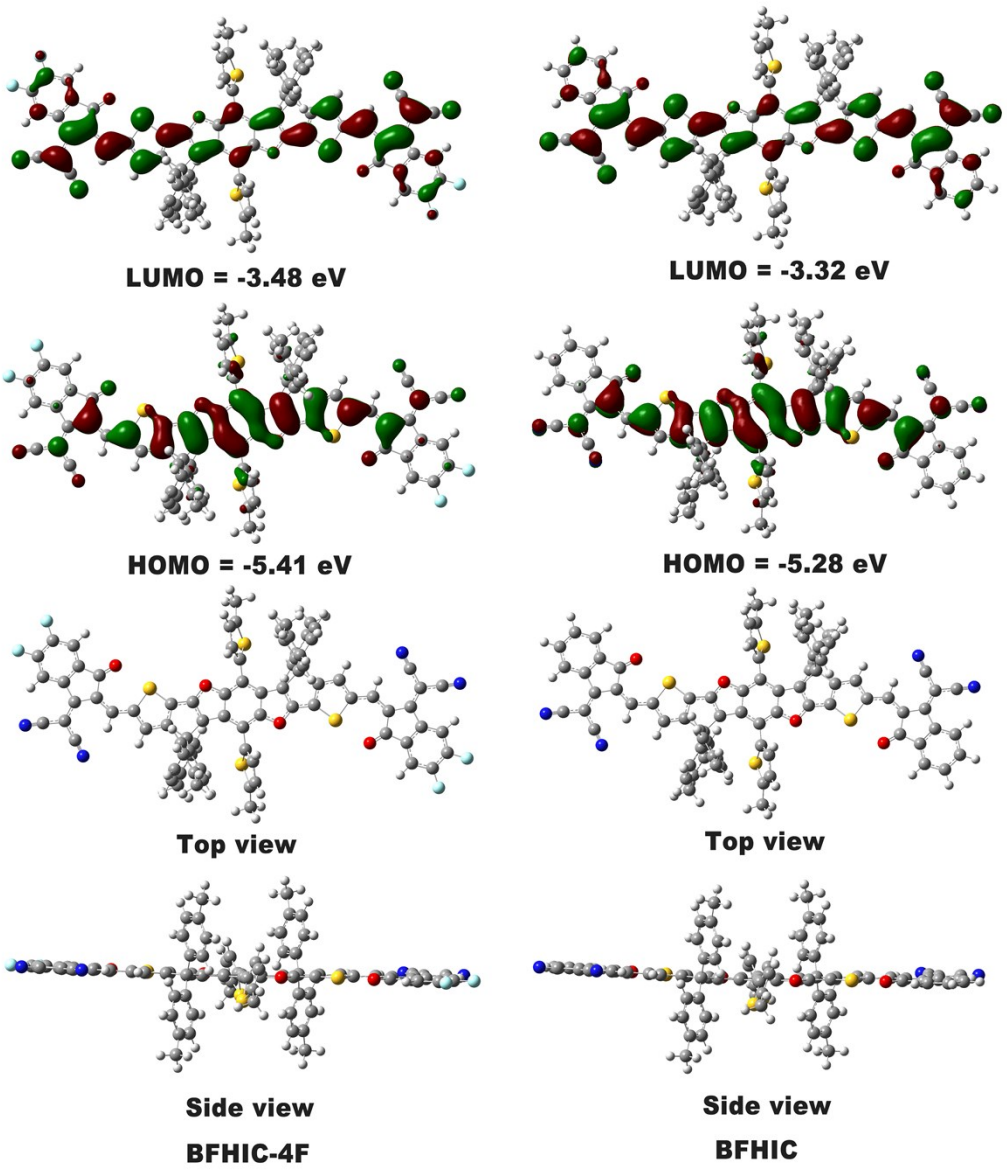

Fig. S13 The frontier molecular orbital (HOMO and LUMO) and optimized geometry of **BFHIC-4F** (left) and **BFHIC** (right) obtained from theoretical calculations by density functional theory (DFT) at the B3LYP/6-31G (d, p) level..

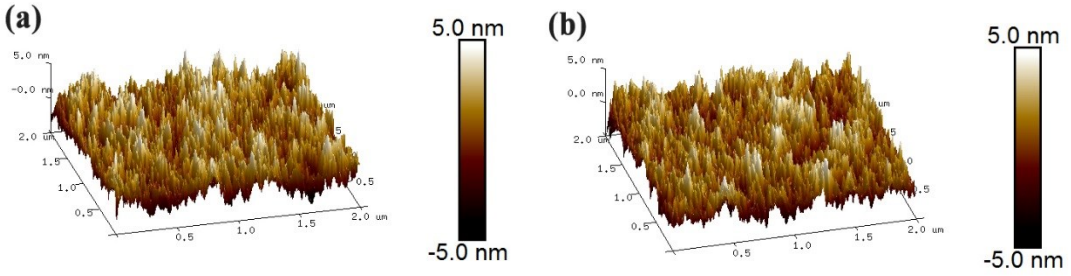

Fig. S14 The AFM images of optimal blend films: (a) three-dimensional height images for PM6:BFHIC-4F; (b) three-dimensional height images for PM6:BFHIC.

Reference

[1] L. Huo, Y. Huang, B. Fan, X. Guo, Y. Jing, M. Zhang, Y. Li and J. Hou, *Chem. Commun.*, 2012, **48**, 3318.

[2] L. Huo, L. Ye, Y. Wu, Z. Li, X. Guo, M. Zhang, S. Zhang and J. Hou, *Macromolecules*, 2012, **45**, 6923.

[3] M. Zhang, X. Guo, W. Ma, H. Ade and J. Hou, *Adv. Mater.*, 2015, **27**, 4655.

[4] C. Liu, D. Zhang, Z. Li, X. Zhang, W. Guo, L. Zhang, S. Ruan and Y. Long, *ACS Appl. Mater. Interfaces*, 2017, **9**, 22068.